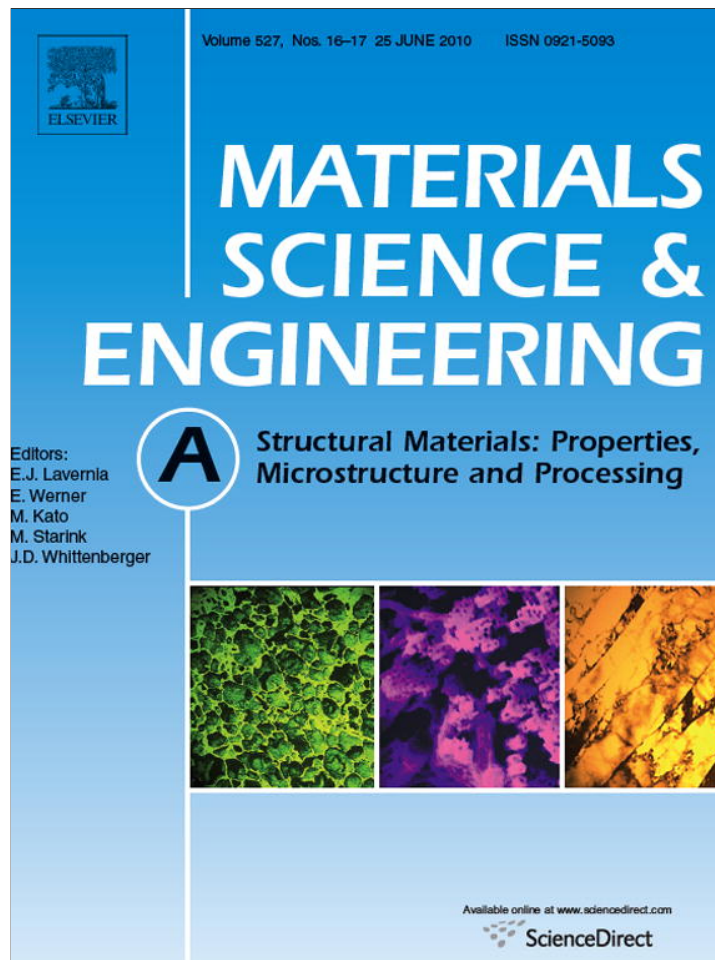


Provided for non-commercial research and education use.
Not for reproduction, distribution or commercial use.



This article appeared in a journal published by Elsevier. The attached copy is furnished to the author for internal non-commercial research and education use, including for instruction at the authors institution and sharing with colleagues.

Other uses, including reproduction and distribution, or selling or licensing copies, or posting to personal, institutional or third party websites are prohibited.

In most cases authors are permitted to post their version of the article (e.g. in Word or Tex form) to their personal website or institutional repository. Authors requiring further information regarding Elsevier's archiving and manuscript policies are encouraged to visit:

<http://www.elsevier.com/copyright>



Contents lists available at ScienceDirect

Materials Science and Engineering A

journal homepage: www.elsevier.com/locate/msea

Microstructural evolution and shear fracture of Cu–16 at.% Al alloy induced by equal channel angular pressing

X.H. An, Q.Y. Lin, S.D. Wu, Z.F. Zhang*

Shenyang National Laboratory for Materials Science, Institute of Metal Research, Chinese Academy of Sciences, 72 Wenhua Road, Shenyang 110016, PR China

ARTICLE INFO

Article history:

Received 10 March 2010

Received in revised form 25 March 2010

Accepted 25 March 2010

Keywords:

Cu–Al alloys

Stacking fault energy (SFE)

Equal channel angular pressing (ECAP)

Microstructure

Shear band

ABSTRACT

Microstructural evolution and shear segmentation of Cu–16 at.% Al alloy with extremely low stacking fault energy (SFE) subjected to multiple-pass equal channel angular pressing (ECAP) were investigated. With increasing plastic deformation, the accommodation of the severe shear strain is transformed from the dislocation slip, stacking faults and deformation twins on the lattice scale to the microshear bands on the grain scale during one- and two-pass ECAP. However, shear fracture happened due to the formation of macroscale shear bands, which can be ascribed to its extremely low SFE leading to the easy saturation of microscale shear bands during plastic deformation during third-pass ECAP. Furthermore, the effects of the SFE on microstructures, grain refinement and shear fracture of various fcc metals were discussed.

© 2010 Elsevier B.V. All rights reserved.

1. Introduction

Ultrafine-grained (UFG) or nanostructured (NC) metallic materials induced by severe plastic deformation (SPD) have been extensively investigated over last decades [1–3]. Various SPD techniques, including equal channel angular pressing (ECAP) [3–8], high pressure torsion (HPT) [2], accumulative roll bonding (ARB) [9], and dynamic plastic deformation (DPD) [10], have been widely developed to produce the UFG or NC materials that can be used in a wide range of structural applications. As one of the most versatile SPD methods, ECAP was utilized to fabricate bulk billets of dense and contamination-free UFG or NC metallic materials with different crystallographic structures including fcc, bcc and hcp crystals [3–5]. During the ECAP process, a severe shear strain is imposed on the sample when it passes through the main shear plane. Since the cross-section geometry is unchanged after pressing, repetitive pressings and different routines can be easily performed in the same sample. Thus, this technique can provide sufficiently high strain to harvest fairly homogeneous structures and extensively refined grains [3].

Significant progresses have been made in profoundly understanding the nature of shear flow and microstructure evolution of the materials during ECAP via theoretical and experimental methods [11,12] by using single-phase materials including monocrystals [13,14], bicrystals [15], polycrystalline metallic materials [16–18] and two-phase alloys [19]. Moreover, previous investigations docu-

mented that the grain refinement processes during ECAP generally originate from the accumulation, interaction, tangling and spatial rearrangement of dislocations in the metals with medium or high stacking fault energy (SFE) [16,17], and the subdivision of original coarse grains is dominantly operated by twin fragmentation in the materials with low SFE [6–8]. Meanwhile, the microscale shear bands play increasingly crucial roles in refining the coarse grains with decreasing the SFE of materials [8]. Compared with the hcp materials with limited number of slip systems which has high potential for segmentation of the billet and multiple cracking [5], the fcc metals and solid solution alloys with good ductility, can be successfully processed by conducting ECAP using a die with an internal angle of 90° at room temperature (RT) [3]. However, catastrophic cracking occurred along the main shear plane at approximately 45° to the exiting direction when the Cu–16 at.% Al alloy with extremely low SFE of about 6 mJ/m² was pressed during third-pass ECAP with Bc route (90° clockwise rotation around the sample axis between the pass) [6]. In order to unveil the main factors resulting in the shear fracture, the microstructure evolution of Cu–16 at.% Al alloy during ECAP will be systematically explored by recourse to the detailed transmission electron microscope (TEM) observations in this study. Moreover, the roles of both the intrinsic property of materials and external deformation factors in the microstructural evolutions, grain refinement and shear fracture will be meticulously analyzed.

2. Experimental procedure

The Cu–16 at.% Al alloy rods were annealed at 800 °C for 2 h to diminish the effect of mechanical processing and obtain homoge-

* Corresponding author. Tel.: +86 24 23971043.

E-mail address: zhfzhang@imr.ac.cn (Z.F. Zhang).

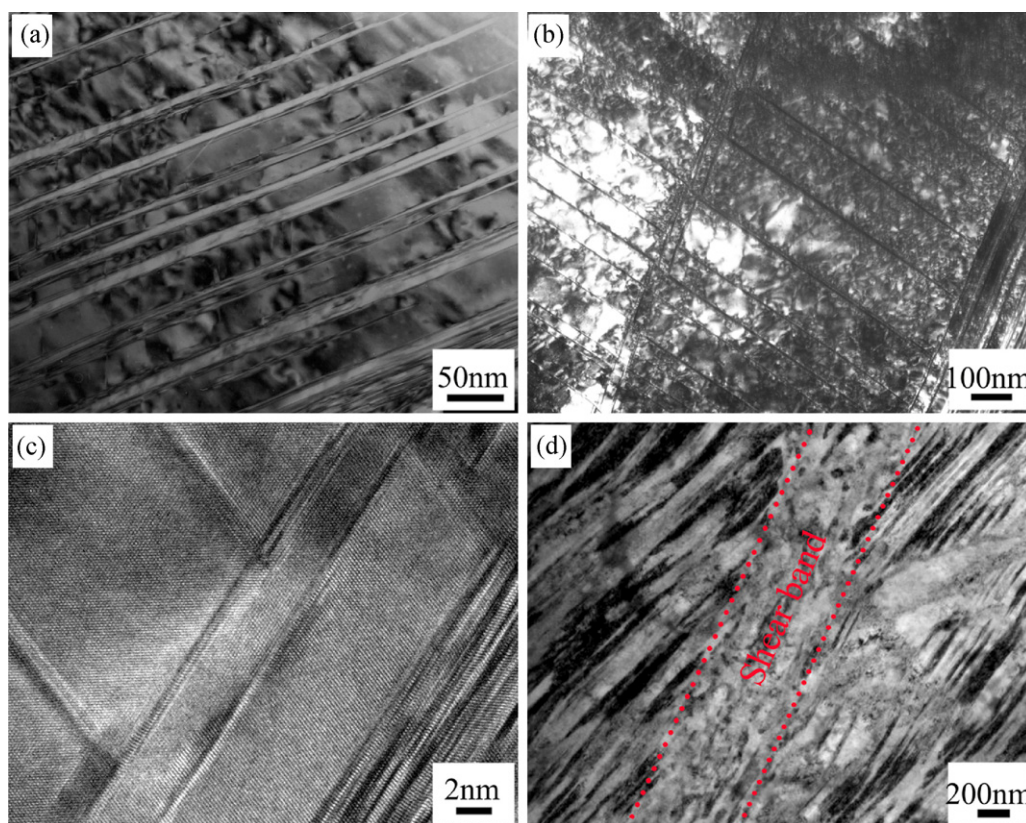


Fig. 1. Microstructures of Cu-16 at.% Al alloy after one-pass ECAP: (a) deformation twins, (b) twin intersections, (c) HRTEM images of deformation twins, stacking faults and twin intersections and (d) microscale shear bands.

neous microstructures with average grain size of approximately $400\ \mu\text{m}$ and the detailed initial microstructures of Cu-16 at.% Al alloy in this work can be found elsewhere [6]. The annealed alloy rods were cut into the samples with 45 mm in length and 8 mm in diameter for ECAP process. The ECAP procedure was performed using a die fabricated from tool steel with two channels intersecting at inner angle of 90° and outer angle of 30° , accordingly, yielding an effective strain of ~ 1 for each pass. All the rods coated with a MoS_2 lubricant were pressed at RT with a pressing speed of 9 mm/min.

After ECAP, the microstructure characterization was performed on TEM (JEM-2010 and FEI Tecnai F20) operated at 200 kV and on FEI Tecnai F30 TEM operated at 300 kV for high-resolution TEM (HRTEM) and the TEM images were taken on a transverse section along the $\langle 110 \rangle$ zone axis. Thin foils for TEM observations, cut from the Y plane (i.e. the flow plane parallel to the side face at the point of exit from the die) [6–8] in the centers of the pressed rods using spark cutting, were first mechanically ground to about $50\ \mu\text{m}$ thick and then thinned by a twin-jet polishing method in a solution of 25% phosphoric acid, 25% ethanol and 50% water with a voltage of 8–10 V at RT. Fracture surfaces of shear fractured Cu-16 at.% Al alloy were also examined in a LEO SUPRA35 scanning electron microscope (SEM) with secondary electron imaging.

3. Experimental results

The characteristic microstructure features of Cu-16 at.% Al alloy after one-pass ECAP are presented in Fig. 1. Profuse thin deformation twins with a thickness of approximately 8–12 nm formed in most grains. In comparison with the twin thickness in Cu and Cu-Al alloys with higher SFE [7,8,17], the thickness of deformation twins greatly decreases due to thin twin embryos and lower growth kinetics of embryos, both of which are controlled by the SFE [20]. Meanwhile, twin intersections are detectable in some grains

favorable for twinning as illustrated in Fig. 1(b). The estimated volume fraction of the twin bundles based on a large number of TEM images is about 60–70%. Based on the HRTEM observations in the Cu-16 at.% Al after one-pass ECAP as exhibited in Fig. 1(c), deformation twins and stacking faults are the main carriers of plastic deformation at a size scale below which the plastic deformation is nonuniform and heterogeneous [21]. However, as a consequence of the nature of ECAP, shear bands, especially in the low-SFE materials, are always found. It is well known that twin boundaries are an effective barrier for piling-up of dislocations which can cause a high stress concentration at the boundaries. Then, twin structures with thin thickness will be destroyed by dislocation breaking through and the localized deformation is created [22,23]. As shown in Fig. 1(d), many microscale shear bands with thickness of about 400 nm traversed the whole grain, implying that localized plastic deformation begins to accommodate severe shear strain on the grain size level. Meanwhile, the nanograins with relatively random orientation were found within each shear bands. The transverse grain size is approximately 50–70 nm and the ratio of longitudinal grain size to transverse size (L/N) is about 3:1 to 4:1.

After two-passes ECAP, as demonstrated in Fig. 2, the density of shear bands was extremely increased and the width of these shear band quickly grew up with the transverse size of about $1.3\ \mu\text{m}$. Moreover, the shear bands intersection can also be found in many regions, as shown in Fig. 2(b). The estimated volume fraction of shear bands is approximately 60%, which signals that shear bands become increasingly dominant deformation mechanism during two-passes ECAP [21]. The transverse grain size of nanograins developed in these shear bands is nearly unchanged, however, the L/N decreases to about 2:1 after two-passes ECAP. This implies that materials within shear bands continue to be deformed with imposing further plastic deformation. Unfortunately, the catastrophic segmentation occurred in the Cu-16 at.% Al alloy subjected

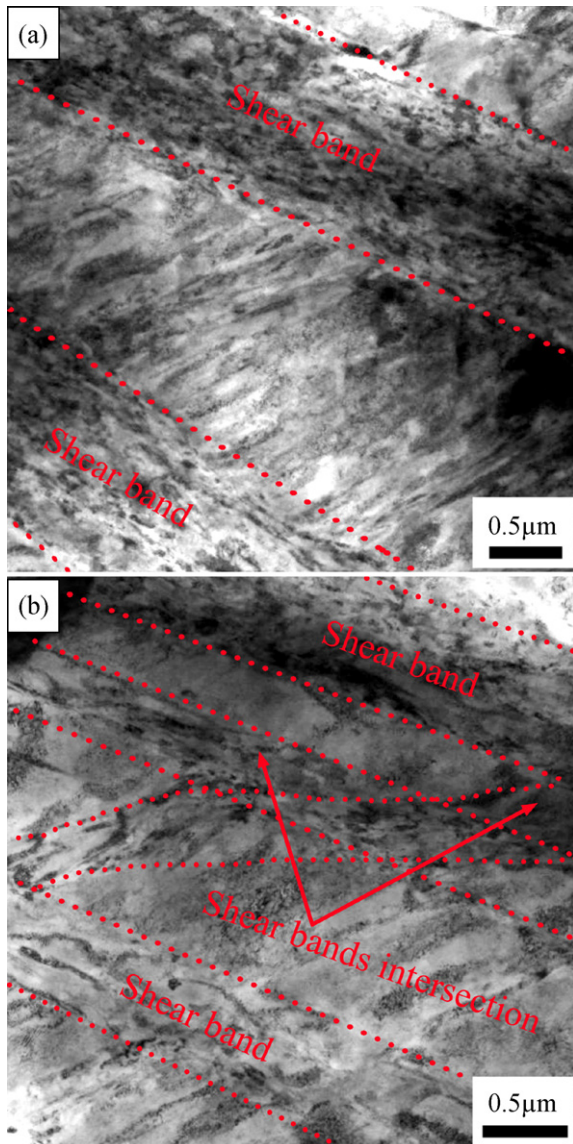


Fig. 2. Microstructures of Cu-16 at.% Al alloy after two-passes ECAP: (a) microshear bands and (b) intersections of microshear bands.

to three-passes ECAP process. Different from the rolling process during which fracture occurs at $\pm 35^\circ$ to the rolling plane [23], shear fracture happened along the main shear plane at approximately 45° to the exiting direction during ECAP, which can be attributed to the different deformation modes. As illustrated in Fig. 3(a) and (b), the fractured samples show the dimple-dominant fracture feature along the shear direction. Meanwhile, the microstructures underneath the fracture surfaces are predominated by the equiaxed nanograins with average grain size similar to the transverse grain size of nanograins formed in the shear bands as shown in Fig. 3(c) and (d). Thus, these equiaxed nanograins may be evolved from the previously formed nanoscale grains and the L/N becomes nearly 1 due to the further deformation and the change of strain path. This also signals that the microscale shear bands are the dominantly typical microstructures of the Cu-16 at.% Al after three-passes ECAP process.

4. Discussions

It is well established that the phenomenon of shear localization is a significant precursor to microcracks due to the presence of

large strain gradient at the band boundaries and macroscale shear bands will lead to fracture when the materials appear to become saturated with a uniform distribution of microscale shear bands [21–24]. Meanwhile, the shear bands in the micro- and macroscale formed more readily with decreasing the SFE of materials [25]. In the case of pure polycrystalline fcc metals with high SFE where the dislocations have high mobility, the shear bands are formed only on a microscopic scale and these microscale shear bands are not instrumental in promoting failure [3,4]. However, in the low-SFE materials whose dislocations activities are relatively limited [25], plastic deformation induced microstructures are significantly fine and the higher strain-hardening rate makes these materials much harder with the plastic deformation. Then, at larger plastic strain, the deformation induced characteristic microstructures will be consumed by the nucleation, propagation and intersection of microscopic shear bands to accommodate further plastic deformation [22]. Moreover, the grain boundaries of the nanograins, formed in the microscale shear bands, are with high density of extrinsic dislocations and lattice distortion near grain boundaries, and then these boundaries originated from SPD are non-equilibrium and have high energy [3]. Therefore, these nanograins will promote appropriate grain rotation which aligns the grain with the most active slip planes leading to macroscopic shear bands [24]. Once a macroscale shear band forms, very little additional overall deformation takes places while large localized strain accumulates in the bands, resulting in the shear fracture or segmentation. Thus, based on the microstructure investigations mentioned above and the previous researches [6–8,21–23], the shear fracture can be ascribed to the formation of macroscopic shear bands during multiple-passes ECAP.

Furthermore, unlike the age-hardenable aluminum alloys where the formation of metastable precipitates limits the deformability of the billets [26], the solid solution atoms in the single-phase Cu-16 at.% Al alloy is not the crucial factor to make the sample be segmented. In addition, for Cu-30 wt.% Zn alloy with a low SFE of 14 mJ/m^2 , it can be still pressed even for four passes successfully [27]; however, Cu-3 wt.% Si alloy with the lowest SFE of 3 mJ/m^2 is also broken into several pieces by shear fracture occurring along macroscopic shear bands at approximately 45° to the pressing axis when subjected to third-pass ECAP [27,28]. Thus, although the solid solution atoms, to some extent, can increase the work hardening rate [25], the SFE may be still the most essential factor in controlling whether the shear fracture occurs or not during ECAP. Moreover, previous documents presented that, apart from the SFE, the characteristics of shear banding was determined by many factors including the method of deformation, strain magnitude, temperature and strain rate [29]. Thus, the external loading conditions also significantly influence the shear fracture induced by the macroscopic shear bands. For the materials with low SFE subjected to the rolling process, the threshold strain magnitude forming the macroscale shear bands is relatively smaller than that in these materials during ECAP [23]. And if the rigorous external deformation conditions are applied, the critical strain for crack formation will be significantly decreased [20]. However, these low-SFE materials, such as Cu-Al [27] alloys and Cu-Zn alloys [30–33], can be successfully processed up to 5 turns without catastrophic failure during HPT deformation with constrained conditions [27]. In fact, by recourse to the previous experiments on the difficult-work materials successfully processed by ECAP, such as Mg, Ti and their alloys, and age-hardenable Al alloys [5,34–36], it is reasonable to expect that the low-SFE materials can also be successfully prepared by multiple-passes ECAP to harvest uniform microstructures without cracking at elevated temperatures or by using a die with a larger channel angle, or using a die equipped with a back-pressure facility. By using these processing strategies [34–36], the severe plastic strain can be distributed

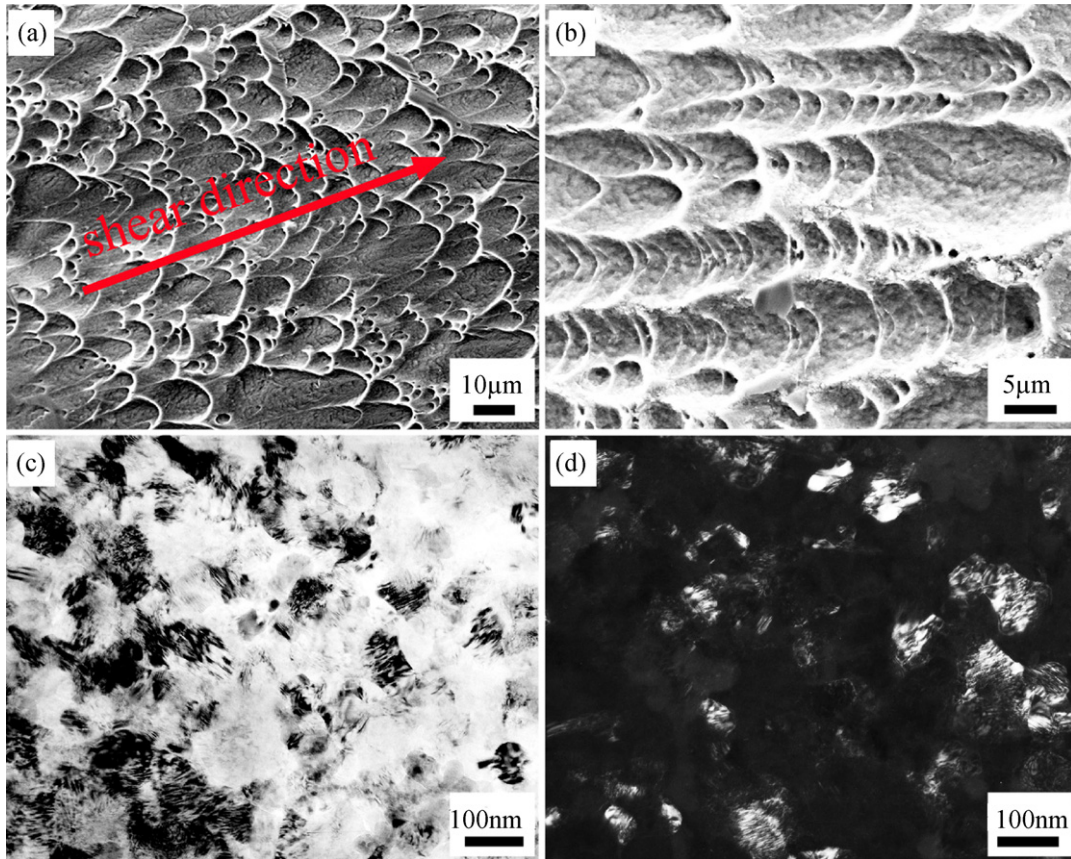


Fig. 3. (a and b) SEM images of fracture surfaces of Cu-16 at.% Al after third-pass ECAP; (c and d) bright and dark filed TEM images of the nanograins formed along the shear fracture plane.

more uniformly in the shear zone, which can delay or prevent the formation of strain localization and then reduce or avoid the propensity for shear cracking and segmentation. Thus, apart from the crucial effect of SFE, external processing conditions also greatly influence the formation of macroscopic shear bands or shear fracture.

In cubic metals, the most intrinsic parameter determining the choice of deformation mechanisms is the value of SFE, which

significantly controls the microstructural evolution and grain subdivision. In combination with the results reported early [27,37–40], the effects of the SFE on the microstructures, grain refinement mechanism and the shear fracture can be summarized in Fig. 4. At low strain level, the influence of the SFE on the microstructures during ECAP is comparable to that during rolling and other deformation modes [22,25]. When these fcc metals are processed at higher strain level, the grain refinement mechanism gradually transformed from

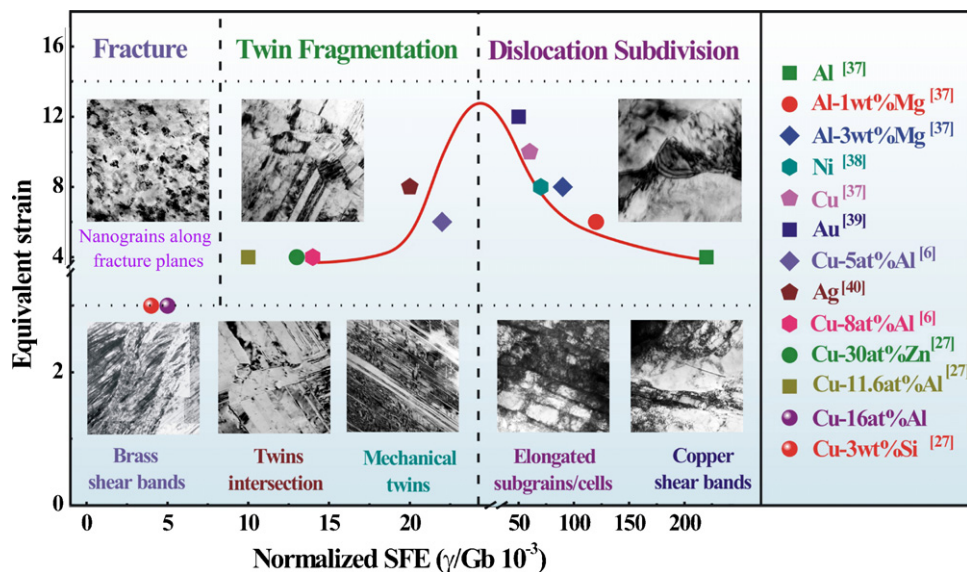


Fig. 4. Effects of SFE on the microstructures, shear fracture, grain refinement and formation of uniform structures in various fcc metals and alloys during ECAP [6,27,37–40].

the dislocation subdivision to the twin fragmentation due to the transition of the deformation mechanisms with decreasing the SFE of materials. For the materials with extremely low SFE, shear segmentation happened due to the formation of macroscopic shear bands although the nanograins formed underneath the fracture surfaces. In addition, the easiness of the homogenous microstructure formation is also crucially influenced by the SFE. As exhibited in Fig. 4, the uniform microstructure of materials with either high or low SFE is much more readily achieved than that of metals with medium SFE during ECAP. For the high-SFE materials, they have a higher rate of recovery due to the strong dislocation activities, resulting in a faster evolution of uniform microstructures. However, deformation twinning transforms the homogeneously deformed fcc metals into a laminar fine structure in the low-SFE metals [28]. The intersections of twins, secondary twins and shear bands will accelerate the formation of nanograins with a uniform distribution [6,41]. Consequently, the formation of uniform microstructures is the most challenging in the medium-SFE materials due to their lower recovery rate of dislocation and the difficulties of the homogeneously twinned structures formation at RT and low strain rate [6,8,17].

5. Conclusions

In summary, with increasing plastic deformation, the accommodation of the severe shear strain is gradually transformed from the dislocation slip, stacking faults and deformation twinning on the lattice scale to the microshear bands on the grain scale in Cu–16at.% Al during multiple-passes ECAP. Due to the easy saturation of microscale shear bands resulted from its extremely low SFE, the macroscopic shear bands are readily formed in this alloy, which will make the billets shear fracture. Meanwhile, in combination with the previous investigations, the grain refinement and microstructures are greatly influenced by the SFE of materials and the uniform microstructures can be readily achieved in the high/low-SFE materials during ECAP.

Acknowledgements

The authors acknowledge gratefully the kind suggestions and valuable discussions with Prof. T.G. Langdon, Prof. S. Mahajan and Prof. M.A. Meyers. This work is supported by the Innovation Fund for Graduate students of IMR.CAS and National Natural Science Foundation of China (NSFC) under grant nos. 50841024 and 50890173, 50931005. Z.F. Zhang would like to acknowledge the financial support by the National Outstanding Young Scientist Foundation under Grant no. 50625103.

References

- [1] M.A. Meyers, A. Mishra, D.J. Benson, *Prog. Mater. Sci.* 51 (2006) 427.
- [2] A.P. Zhilyaev, T.G. Langdon, *Prog. Mater. Sci.* 53 (2008) 893.
- [3] R.Z. Valiev, T.G. Langdon, *Prog. Mater. Sci.* 51 (2006) 881.
- [4] S.D. Wu, X.H. An, W.Z. Han, S. Qu, Z.F. Zhang, *Acta Metall. Sin.* 46 (2010) 257.
- [5] R.B. Figueiredo, P.R. Cetlin, T.G. Langdon, *Acta Mater.* 55 (2007) 4769.
- [6] S. Qu, X.H. An, H.J. Yang, C.X. Huang, G. Yang, Q.S. Zang, Z.G. Wang, S.D. Wu, Z.F. Zhang, *Acta Mater.* 57 (2009) 1586.
- [7] X.H. An, W.Z. Han, C.X. Huang, P. Zhang, G. Yang, S.D. Wu, Z.F. Zhang, *Appl. Phys. Lett.* 92 (2008) 201915.
- [8] X.H. An, Q.Y. Lin, S. Qu, G. Yang, S.D. Wu, Z.F. Zhang, *J. Mater. Res.* 24 (2009) 3636.
- [9] Y. Saito, H. Utsunomiya, N. Tsuji, T. Sakai, *Acta Mater.* 47 (1999) 579.
- [10] Y.S. Li, N.R. Tao, K. Lu, *Acta Mater.* 56 (2008) 230.
- [11] W.Z. Han, Z.F. Zhang, S.D. Wu, S.X. Li, *Mater. Sci. Eng. A* 476 (2008) 224.
- [12] W.Z. Han, Z.F. Zhang, S.D. Wu, S.X. Li, *Philos. Mag. Lett.* 87 (2007) 735.
- [13] W.Z. Han, Z.F. Zhang, S.D. Wu, S.X. Li, *Acta Mater.* 55 (2007) 5889.
- [14] W.Z. Han, Z.F. Zhang, S.D. Wu, C.X. Huang, S.X. Li, *Adv. Eng. Mater.* 10 (2008) 1110.
- [15] W.Z. Han, H.J. Yang, X.H. An, R.Q. Yang, S.X. Li, S.D. Wu, Z.F. Zhang, *Acta Mater.* 57 (2009) 1132.
- [16] Y. Iwahashi, Z. Horita, M. Nemoto, T.G. Langdon, *Acta Mater.* 45 (1997) 4733.
- [17] C.X. Huang, K. Wang, S.D. Wu, Z.F. Zhang, G.Y. Li, S.X. Li, *Acta Mater.* 54 (2006) 655.
- [18] C.X. Huang, G. Yang, Y.L. Gao, S.D. Wu, S.X. Li, Z.F. Zhang, *Philos. Mag.* 87 (2007) 4949.
- [19] Y.Z. Tian, W.Z. Han, H.J. Yang, H.F. Zou, S.D. Wu, Z.F. Zhang, *Scr. Mater.* 62 (2010) 183.
- [20] Y. Zhang, N.R. Tao, K. Lu, *Scr. Mater.* 60 (2009) 211.
- [21] R.J. Asaro, A. Needleman, *Scr. Metall.* 18 (1984) 429.
- [22] M. Hatherly, A.S. Malin, *Met. Technol.* 6 (1979) 308.
- [23] M. Hatherly, A.S. Malin, *Scr. Metall.* 18 (1984) 449.
- [24] A.A.S. Mohammed, E.A. El-Danaf, A.A. Radwan, *J. Mater. Proc. Technol.* 186 (2007) 14.
- [25] M.A. Meyers, K.K. Chawla, *Mechanical Behavior of Materials*, Prentice Hall, New Jersey, 1999.
- [26] N.Q. Chinh, J. Gubicza, T. Czepe, J. Lendvai, C. Xu, R.Z. Valiev, T.G. Langdon, *Mater. Sci. Eng. A* 516 (2009) 248.
- [27] X.H. An, unpublished work.
- [28] W.Z. Han, Z.F. Zhang, S.D. Wu, S.X. Li, *Philos. Mag.* 88 (2008) 3011.
- [29] H. Paul, J.H. Driver, Z. Jasienski, *Acta Mater.* 50 (2002) 815.
- [30] Y.H. Zhao, X.Z. Liao, Y.T. Zhu, Z. Horita, T.G. Langdon, *Mater. Sci. Eng. A* 410 (2005) 188.
- [31] T. Ungár, L. Balogh, Y.T. Zhu, Z. Horita, C. Xu, T.G. Langdon, *Mater. Sci. Eng. A* 444 (2007) 153.
- [32] Y.H. Zhao, Y.T. Zhu, X.Z. Liao, Z. Horita, T.G. Langdon, *Mater. Sci. Eng. A* 463 (2007) 22.
- [33] L. Balogh, T. Ungár, Y.H. Zhao, Y.T. Zhu, Z. Horita, C. Xu, T.G. Langdon, *Acta Mater.* 56 (2008) 809.
- [34] D.P. DeLo, S.L. Semiatin, *Metall. Mater. Trans. A* 30 (1999) 1391.
- [35] X.C. Zhao, W.J. Fu, X.R. Yang, T.G. Langdon, *Scr. Mater.* 59 (2008) 542.
- [36] V.V. Stolyarov, R. Lapovok, I.G. Brodova, P.F. Thomson, *Mater. Sci. Eng. A* 357 (2003) 159.
- [37] S. Komura, Z. Horita, M. Nemoto, T.G. Langdon, *J. Mater. Res.* 14 (1999) 4044.
- [38] A.P. Zhilyaev, B.K. Kim, J.A. Szpunar, M.D. Baró, T.G. Langdon, *Mater. Sci. Eng. A* 391 (2005) 377.
- [39] J. Gubicza, N.Q. Chinh, J.L. Lábár, Z. Hegedűs, C. Xu, T.G. Langdon, *Scr. Mater.* 58 (2008) 775.
- [40] A.V. Nagasekhar, T. Rajkumar, D. Stephan, Y. Tick-Hon, R.K. Guduru, *Mater. Sci. Eng. A* 524 (2009) 204.
- [41] N.R. Tao, K. Lu, *Scr. Mater.* 60 (2009) 1039.